3-D numerical modelling of stresses around a longwall panel with top coal caving

by N.E. Yasitli* and B. Unver*

Synopsis

There is a considerable amount of lignite reserve in the form of thick seams in Turkey. It is rather complicated to predict the characteristics of strata response to mining operation in thick seams. However, a comprehensive evaluation of ground behaviour is a prerequisite for maintaining an efficient production, especially when top coal winning by means of caving behind the face is applied. A comprehensive modelling of deformations and induced stresses is vital for the selection of optimum production strategy. In this study, numerical modelling and analysis of a longwall panel at Omerler underground coalmine have been carried out by using the software called FLAC3D developed based on the finite difference technique. Firstly, a 3-D numerical model of the M3 panel has been prepared. Secondly, induced stresses formed around the longwall face have been determined as a function of face advance where the face was located at the bottom of thick coal-seam. Results obtained from modelling studies have revealed that the front abutment vertical stress was maximum at 7 metres in front of the face and magnitude of front abutment stress was found to increase up to a distance of 200 metres away from the face start line. As the face was further advanced after 200 m from the face start line, there was not any significant change in the characteristics of front abutment stresses. Results of numerical analysis of the panel were in good agreement with *in situ* observations.

Introduction

Evaluation of ground response during longwall mining is a rather difficult task due to its dynamic nature. Loading characteristics around face and gate roadways change continuously depending on production activity. In this sense, it is not possible to consider only static loading conditions to fully understand the strata behaviour. Hence, dynamic loading resulting from the caving ground behind the face must be taken into account.

Assessment of strata response to production is relatively easy for conventional single slice longwall mining. However, in the case of thick seam mining, it is a more difficult task to assess ground movements due to successive caving if slicing or caving of top coal behind the face methods are applied.

A better understanding of strata behaviour under existing conditions would facilitate the selection and application of an efficient production strategy. This cannot be accomplished by an analytical solution due to difficulty in modelling of the complex structure around a longwall panel. Physical models may be used to a certain extent; however, it is a rather laborious, expensive and time-consuming method. Therefore, physical modelling is not a practical method.

Availability of computers having high-speed processors and increased storage capacity has enabled a more realistic modelling of underground structures in 3-D. A 2-D analysis is not adequate for inclusion of necessary details in the model. Therefore, a realistic analysis of stress and displacements around a longwall panel can only be modelled by 3-D numerical solutions. In this study, a numerical model of the M3 longwall panel at Omerler underground mine has been formed in 3-D by using a commercially available software called FLAC3D. Change of stress distributions depending on the face advance has also been determined.

A Brief information on Tuncbilek District and Omerler underground mine

Tuncbilek District is located in the inner Aegean district of Turkey near Kutahya Province (Figure 1). It is 13 km from Tavsanli and 63 km from Kutahya. The total proven lignite reserve in the district is around 330 million tons. The proven reserves suitable for underground and surface production are 263 million and 67 million tons, respectively. Average calorific value of lignite in Tuncbilek District is 4500 kcal/kg with an average sulphur content of 2%.

Coal production is performed from both opencast and underground mines in the district. While stripping is performed with

* *Hacettepe University, Department of Mining Engineering, Ankara, Turkey.*

 SA ISSN 0038–223X/3.00 + 0.00. Paper received Sep. 2004; revised paper received Feb. 2005.

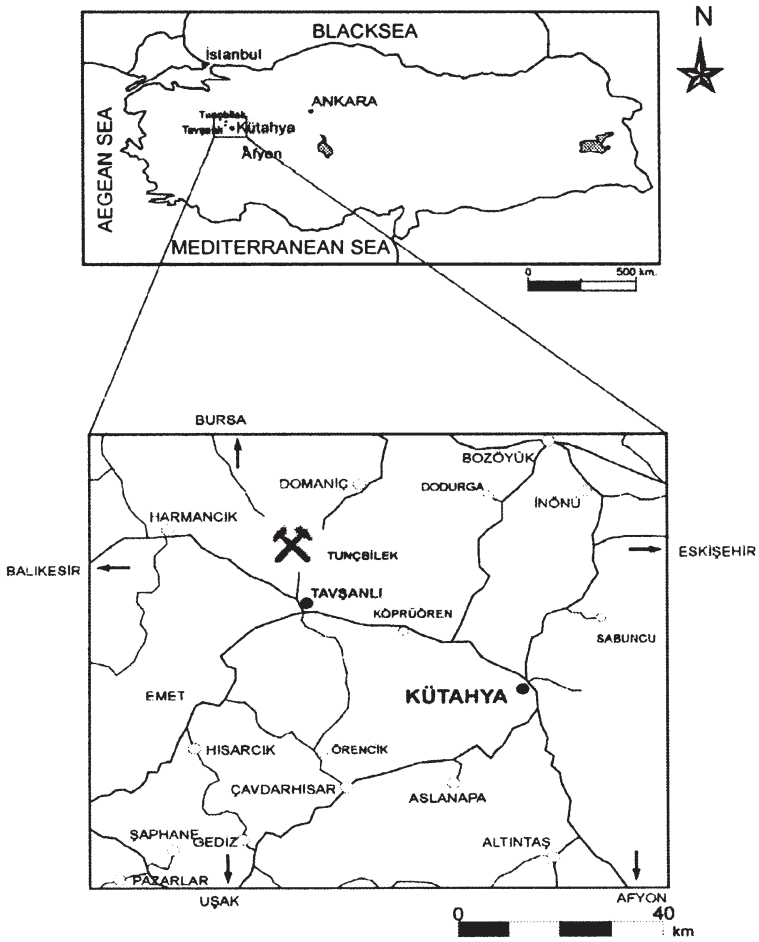

Figure 1—Location map of GLI region (Tuncbilek)

excavator-truck and dragline systems, coal is produced with an excavator-truck system at opencast mines. Underground coal production is performed at two distinct underground mines, Tuncbilek and Omerler. Coal is produced by a conventional longwall retreat with top coal caving production method in Tuncbilek mine and by fully a mechanized retreat with top coal caving production method in Omerler mine. Produced coal is cleaned and sized at Tuncbilek and Omerler coal washery. There are three power plants with a total capacity of 429 MW in the district.

Production started at Omerler underground mine in 1985 by the retreat longwall with top coal caving method. A conventional support system was used until 1997 in the mine and a fully mechanized face was established in 1997. Average depth below surface was around 240 m and the 8 m thick coal-seam had a slope of 10°. As seen in Figure 2, six panels were planned for extraction by means of the fully mechanized face in sector A. At the time of this study, two adjacent longwall panels, namely M1 and M2, had been completed and the production was being carried out at M3 panel as shown in Figure 2. Coal has been produced by means of the longwall retreat with top coal caving production method where a 2.8 m high longwall face was operated at the floor of the coal-seam (Figure. 3). Top slice coal having a thickness of 5.2 m was caved and produced through windows located at the top of shields.

In order to determine the geological units and geotechnical parameters of these units in the region, drilling was performed and tuff, limestone, sandstone, conglomerate, serpentine, peridotite, claystone, dolomite, magnetite, calcareous marl and marl were crossed. The geological units fall into 3 main groups as shown in Figure 4. Physical and mechanical parameters of surrounding rocks and the coal seam are presented in Table I[1–3]. A laboratory test programme was carried out on the samples taken from the hangingwall, footwall, roof and floor of the coal at Omerler M3 panel and the results are also presented in Table I .

Numerical modelling

Modelling procedure with FLAC3D in general

FLAC3D is widely used numerical software for stress and deformation analysis around surface and underground structures opened in both soil and rock. The software is based on the finite difference numerical method with Lagrangian calculation. The finite difference method can be applied better to modelling stress distribution around underground mining excavations in comparison to other numerical techniques. FLAC3D is a commercially available software that is capable of modelling in three dimensions.

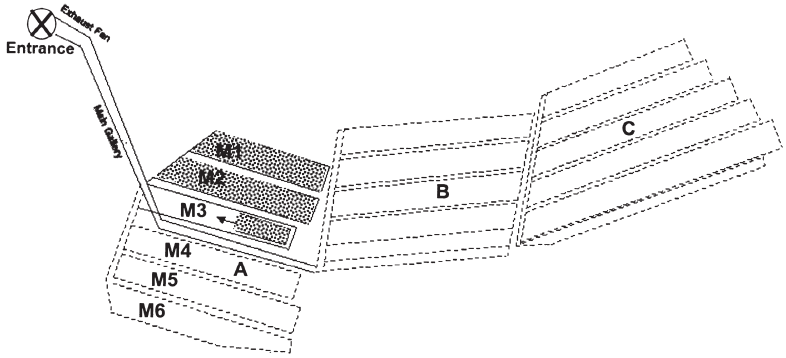

Figure 2—A simplified plan view of Omerler underground mine

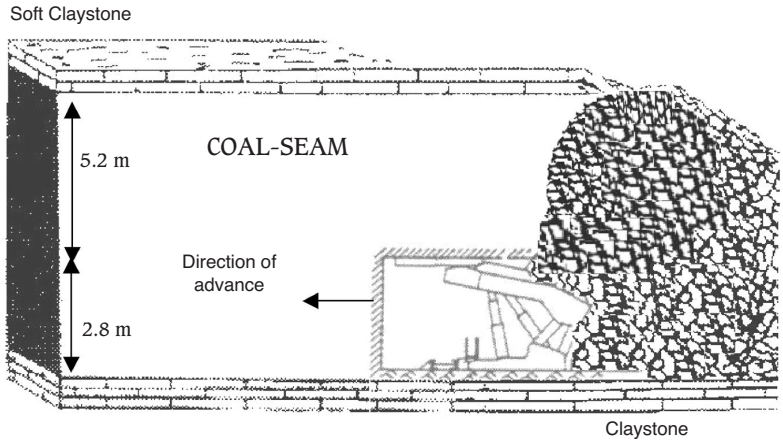

Figure 3—Longwall with top coal caving method as applied at Omerler underground mine

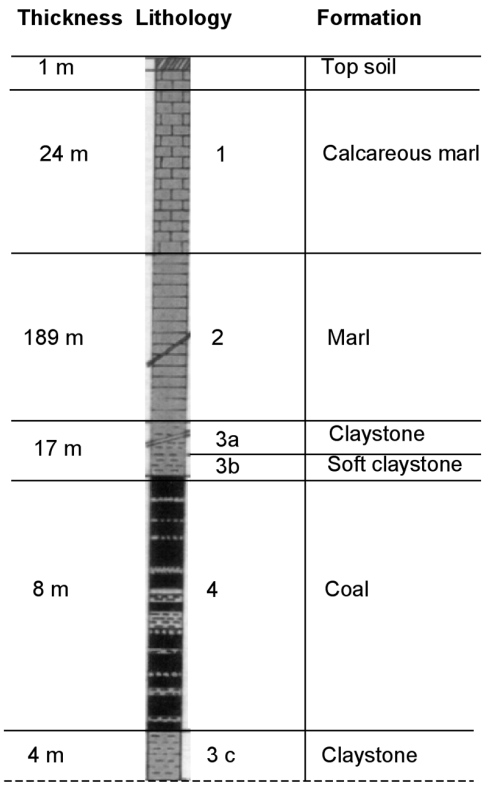

Figure 4—A generalized stratigraphic column at Omerler coalmine

Table I

Physical and mechanical properties of coal and surrounding rocks[1–3]

Formation	Density (MN/m3)	Porosite (%)	Uniaxial compressive strength (MPa)	Tensile strength (MPa)	Internal friction angle (ϕ)	Cohesion c (MPa)	Modulus of elasticity E (MPa)	Poisson's ratio ν
Calcareous marl	0.023	13.8	29.2	3.9	47	12.5	5520	0.26
Marl	0.022	-	16.1	1.9	31	5.0	2530	0.25
Roof claystone	0.021	21.30	14.4	2.3	32	3.18	1480	0.28
Soft claystone	0.023	10.8	8.7	1.8	15–35	-	2040	-
Floor claystone	0.024	21.30	26.5	3.5	40	2.90	2085	0.31
Coal	0.013	9.72	15.9	-	15–25	-	1733	0.25

Modelling for estimation of stresses around the longwall panel is performed in five steps. The steps called A, B, C, D and E are as follows:

A—Determination of boundaries and material properties
B—Formation of the model geometry and meshing
— Determination of the model behaviour
C—Determination of the boundary and initial conditions
— Initial running of the program and monitoring of the model response
D—Re-evaluation of the model and necessary modifications
E—Obtaining the results.

Model geometry and meshing

Model geometry and meshing refer to the physical conditions of the district to be modelled. Model behaviour is considered to be the response of a model under a certain loading condition. By means of boundary and initial conditions, physical limits of the model and original conditions are explained. At the beginning of analysis, the model was in the form of a solid block in which gate roadways, the face and other structures were later created in the form of modifications. The modelling process is presented in Figure 5 in the form of a flowsheet[4]. Details of the modelling geometry are presented in Figure 6.

Steps of a true scale 3-D modelling of M3 longwall panel with FLAC3D are given below:

- The face length was 90 m at M3 longwall panel. Therefore, the face length was taken as 90 m in the $+x$ coordinate axis in the model.
- The actual panel length was 450 m. However, due to computer running time and capacity restrictions, the panel length was taken as 250 m in the $+y$ coordinate axis in the model.
- In accordance with the actual depth below surface, this value was taken as 240 m in the $-z$ coordinate axis in the model.
- There was a mined-out panel called M2 separated by a 16 m wide rib pillar. the rib pillar and mined-out area were both included in the model.
- In order to obtain better stress distribution results, a smaller mesh size was selected at regions in the vicinity of the production region.
- Coal cut from the face and caved behind the face was divided into 3 and 5 meshes, respectively.
- The completed model was run by assuming a gravitational loading condition. the magnitudes of stresses in different directions as a result of gravitational loading were calculated.

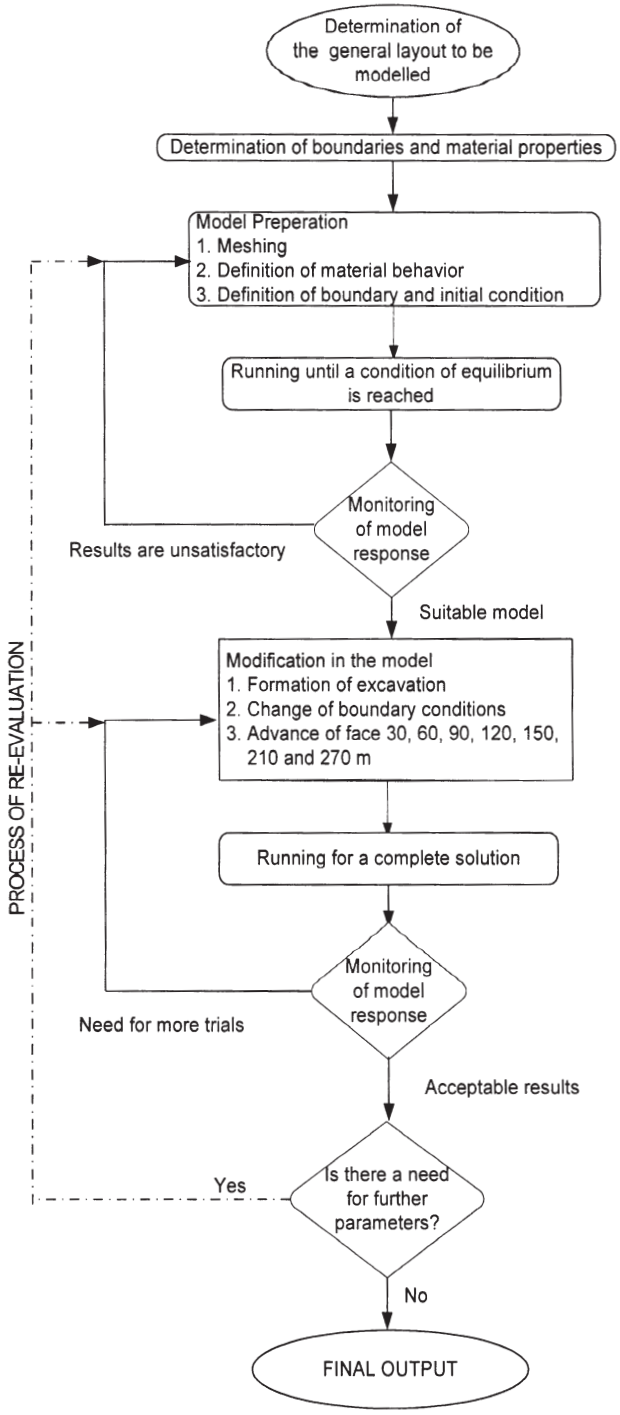

Figure 5—A general flowsheet of modelling process[3,4,11]

➤ Cubic and prismatic (brick) elements were used for model construction. The model was composed of 16 524 elements and 18 648 gridpoints as shown in Figure 6.

An assessment of material properties and rock mass strength

It is crucial to properly assess material properties in order to obtain acceptable results in modelling with FLAC3D. Therefore, the physical and mechanical properties of each geological unit must be properly determined. In general, intact rock properties are determined by means of laboratory testing. However, there is an important difference between rock material and rock mass characteristics. It is compulsory to determine representative physical and mechanical properties of the rock mass instead of intact rock material.

Data regarding the physical and mechanical properties of surrounding rock given in Table I were obtained by testing carried out on core samples obtained from exploration drilling and rock blocks taken directly from the mine. Therefore, the data presented in Table I are representative of only rock material. It is a rather difficult task to determine rock mass strength characteristics. Therefore, it is a common practice to derive rock mass strength from rock material properties by using various failure criteria. In this study, rock material properties were converted into rock mass data by using empirical relationships widely used in the literature, i.e. Hoek and Brown[5] failure criterion, Bieniawski's[6,7] RMR classification system and Geological Strength Index (GSI)[8–10]. The physical and mechanical properties of rock mass used for modelling are presented in Table II[3,11,12].

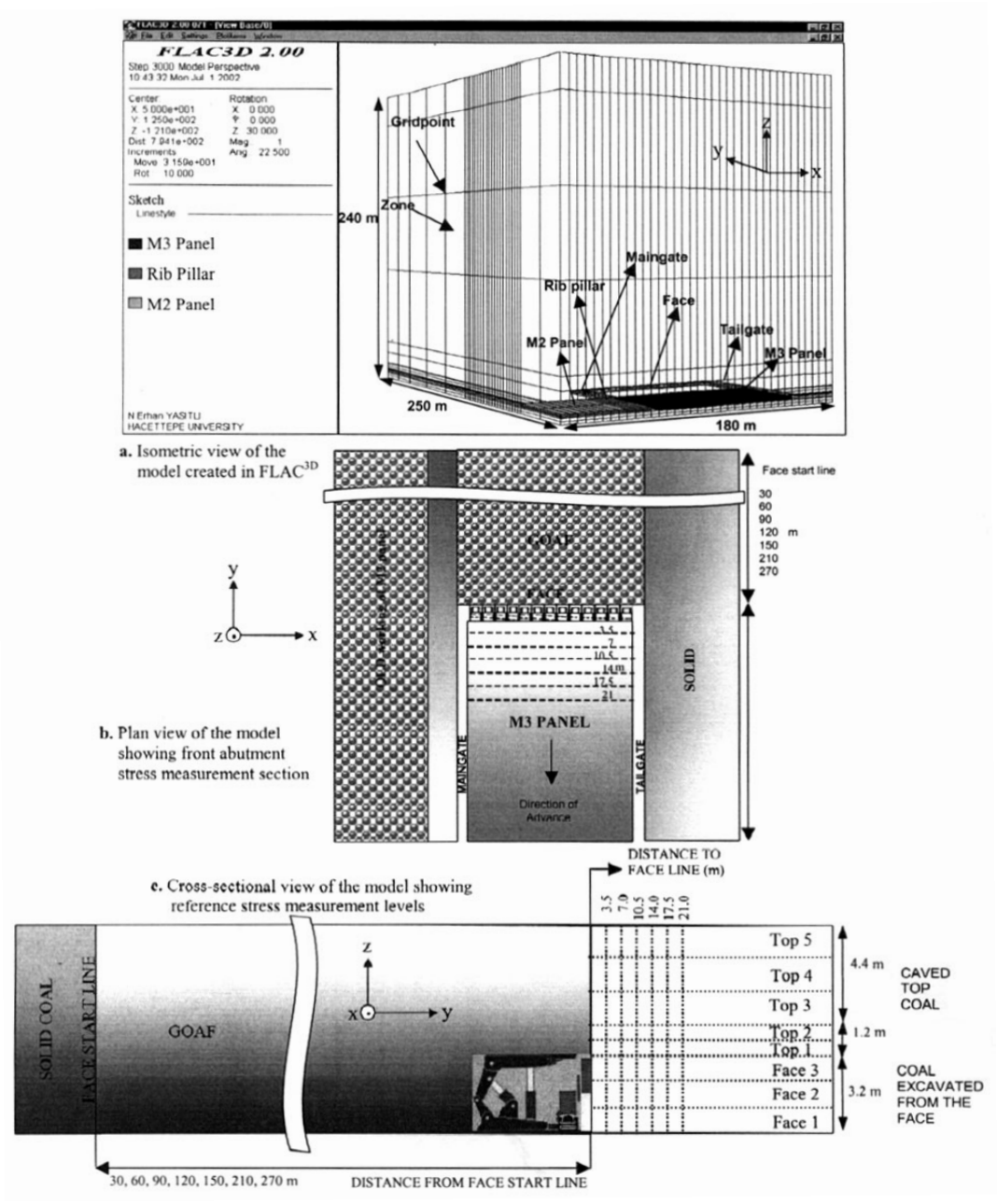

Figure 6—Details of model geometry of Omerler underground mine

Table II

The input parameters regarding rock mass used in numerical modelling[3,12]

Rock definition	Unit	Calcareous marl	Marl	Roof claystone	Soft claystone	Coal	Floor claystone
Density (d)	(MN/m3)	0.023	0.022	0.025	0.023	0.014	0.027
Internal friction angle (ϕ)	(°)	27.5	24.8	18.8	14.0	21.8	18.4
Cohesion (c)	(MPa)	1.3	0.65	0.41	0.167	0.517	0.715
Modulus of elasticity (E)	(MPa)	3404	1420	921	746	955	1375
Tensile strength	(MPa)	0.096	0.074	0.031	0.006	0.017	0.035
Poisson's ratio (ν)	-	0.25	0.25	0.28	0.25	0.25	0.31
Bulk Modulus* (K)	(MPa)	2269	947	698	497	637	1206
Shear Modulus** (G)	(MPa)	1362	568	360	298	382	525
Uniaxial compressive strength	(MPa)	1.80	1.849	1.131	0.428	1.294	1.981

$$* K = \frac{E}{3(1-2\nu)}$$

$$** G = \frac{E}{2(1+\nu)}$$

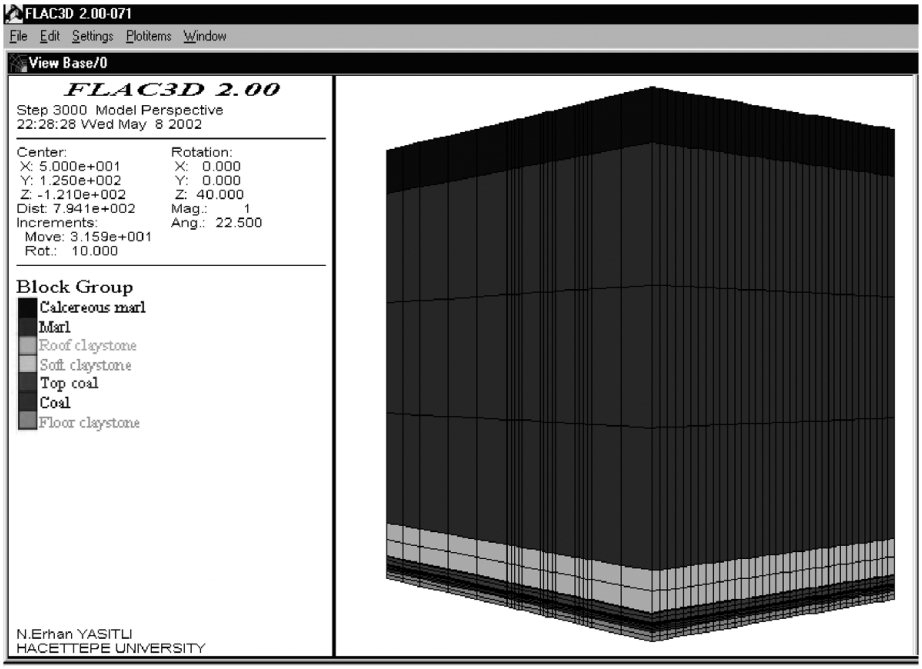

Figure 7—Settings of boundary and initial condition

Determination of goaf material properties

Modelling of the caved area is another important step that affects the accuracy of obtained results. It is a well-known fact that it is a rather difficult task to model goaf material in numerical analysis. Since goaf is mainly made of broken rock pieces, its deformational properties are rather complex due to an ongoing consolidation process with an increase in the amount of load. Xie *et al.*[13] suggested the following formula for determining the modulus of elasticity of goaf material with respect to time:

$$E = 15 + 175\left(1 - e^{-1.25t}\right) \text{ MPa}$$

where t is time in seconds.

This approach was employed for estimating the elasticity (E) modulus of goaf at the beginning (t=0). The E of goaf at the later stages was found by the expression by Kose and Cebi[14] that suggested a wide interval such as 15–3500 MPa for the modulus of elasticity value for goaf material, whereas Yavuz and Fowell[15] suggested a Poisson's ratio of 0.495 for goaf material for the Tuncbilek Region. These values were used for the characterization of goaf material throughout the analyses by assuming a swelling factor for goaf material of 1.5. The modulus of elasticity of goaf material just after caving was taken as 15 MPa. This value was consecutively increased as suggested in the literature by considering the compaction of goaf. At the final stage of analysis, the modulus of elasticity of goaf material was taken as 3500 MPa. Hence, change in the mechanical characteristics of goaf material due to compaction within time and face advance was taken into account.

Setting of boundary and initial conditions

After preparation of the model as given in Figure 6, in order to prevent displacements at the beginning, the right-hand side and left-hand side of the model in $+x$ and $-x$ directions, the front, back and bottom of the model were fixed in $+y$, $-y$ and $-z$ directions respectively (Figure 7).

Formation of underground structures in the model

After setting of boundary and initial conditions, the model that was made of only solid rock mass, not including any openings inside, was solved with gravitational force until a state of equilibrium was reached. After this stage, the model was ready for inclusion of underground mine structures such as roadways and the longwall panel. At first, the maingate and tailgate of M3 panel were formed in the model with their actual dimensions of 4 m in width and 3 m in height. The location of the maingate and tailgate together with the rib pillar left between the M2 old working and M3 panel and the face can be seen in Figure 6. In the mine, the maingate and tailgate were supported by means of rigid steel arches. However, it was not possible to add such a support type in the model prepared by using FLAC3D. Therefore, it was found convenient to represent supporting in the form of a thin layer of shotcrete as structural shell element. Following the formation of the maingate and tailgate, the longwall face was formed. Actual shield supports of the face were modelled in the form of structural shell elements as in the gate roadways. The dimensions of the face were 4 m in height and 3.2 m in width.

The main structure of the model was completed and the model was solved to find stress distribution and displacements. The main purpose of the study was to find changes in stress distribution depending on face advance. Therefore the characteristics of stress distributions were found after a stepwise modelling of face advance as 30, 60, 90, 120, 150, 210 and 270 m from the face start line. Face advance was accomplished in the form of defining goaf material after each step of face advance as given earlier.

Presentation of modelling results

As a result of stepwise modelling depending on face advance, stress and displacement distributions were calculated under various conditions. Horizontal stress distribution in *x* and *y* axes and vertical stress distribution in *z* axis are presented in Figures 8 and 9 after a face advance of 30 m from the face start line. The distribution of vertical stresses in front of the face at various distances towards the direction of advance from the face line such as 3.5, 7, 10.5, 14, 17.5 and 21 metres at eight different levels (see Figure. 6) of the coal-seam at every 5 m starting from maingate towards tailgate are presented in Figure 10.

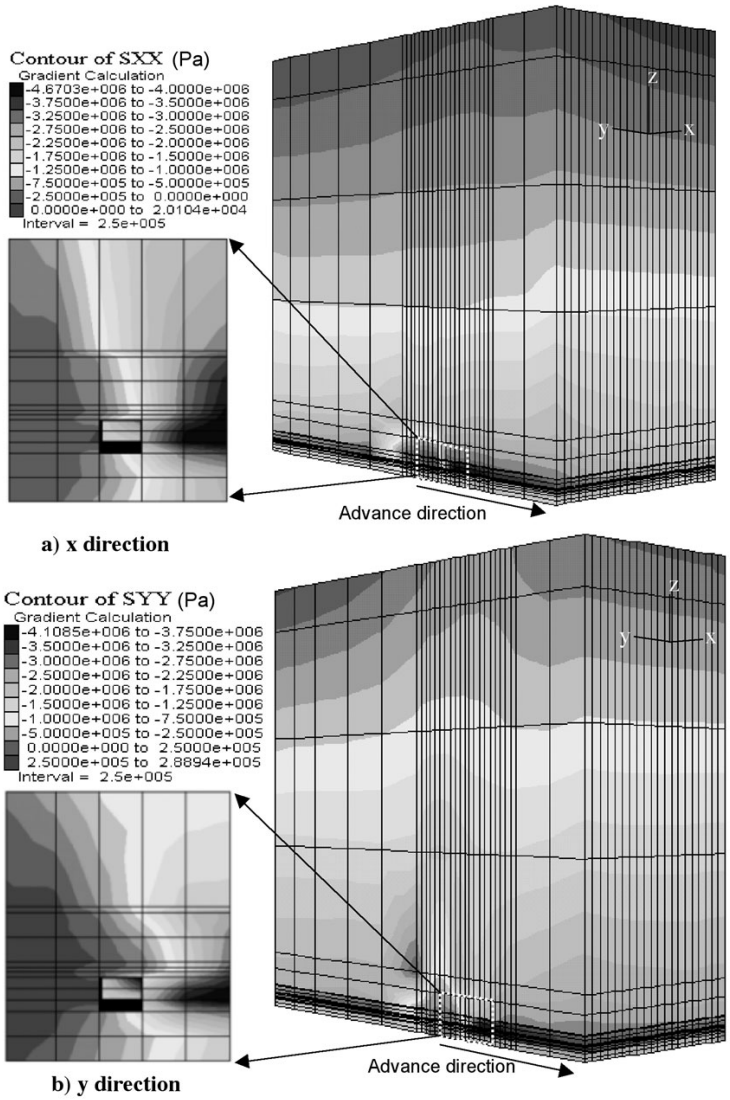

Figure 8—Distribution of horizontal stresses (x and y direction) after 30 m of face advance

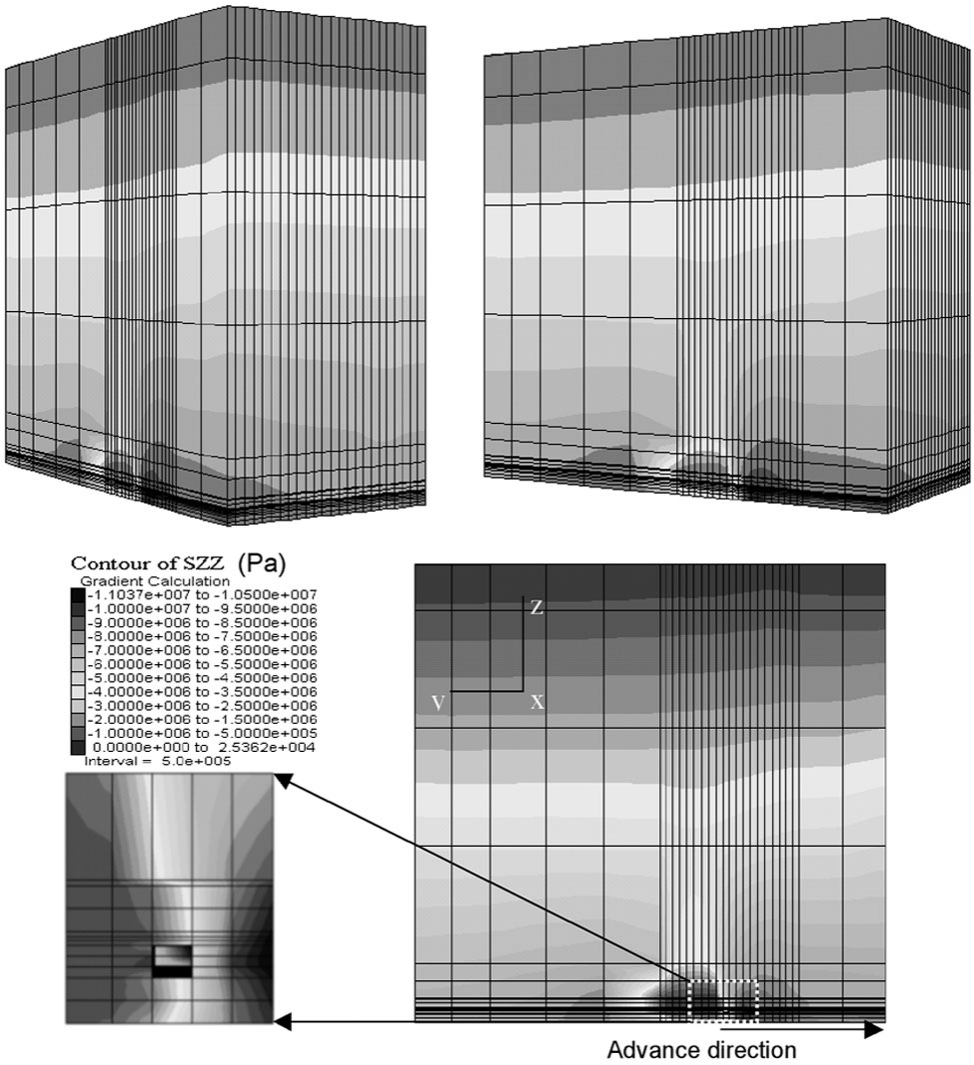

Figure 9—Vertical stresses distribution (z direction) after 30 m of face advance

In order to obtain stress distribution in a categorized form, the 8.8 m thick coal seam was divided into 3 levels at the face and 5 levels at the top coal (see Figure. 6).

Calculated maximum horizontal stresses were in the order of 4.67 MPa in *x* direction and 4.10 MPa in the *y* direction at 7 m in front of the face. Maximum vertical stress at the same region was found as 11.80 MPa. The model was modified after each run to find the effect of 60, 90, 120, 150 m of face advance to determine the corresponding change in stress distributions. The change in the magnitude and distribution characteristics of vertical stress with face advance can be seen from Figures 11, 12, 13 and 14 on a comparative basis. As shown in the Figure 15, calculated horizontal stresses increased from 4.67 to 5.36 MPa in *x* direction, from 4.37 to 4.90 MPa in the *y* direction and vertical stress increased from 11.30 to 14.40 MPa in the *z* direction at 7 m in front of the face depending on face advance. Results revealed that *z*, *x* and *y* directions correspond to maximum, intermediate and minimum principal stress directions, respectively.

Vertical stress distributions parallel to the face at a distance of 3.5, 7, 10.5, 14, 17.5 and 21 m ahead of the face are presented in Figure 15. As a result of modelling studies, after 60, 90 and 150 m of face advance, the maximum vertical stresses formed between 30–50 m inside from the maingate approximately at the centre region of the face and after 120 m of face advance, whereas the vertical stresses were maximum in the region between 20–35 m inside from the maingate. An analysis of calculated vertical stresses by means of modelling has revealed that at a distance of 7 m ahead of the face, vertical stresses reached to a maximum.

Evaluation of modelling results

Stress distribution around longwall faces has been studied by various researchers depending on *in situ* measurements[16–18]. As it can be seen in Figure 16, vertical stress increases in front of the face and gradually decreases to a value equal to field stress at a distance about 0.12 times depth below surface in front of the face. Following the eventual failure of the coal-seam in the maximum front abutment region, maximum stress would tend to shift a couple of metres away ahead of the face. On the other hand, vertical stress drastically drops to zero at coal-seam roof contact and then a gradual build-up of vertical stress is observed in the goaf region behind the face, depending on the rate of compaction.

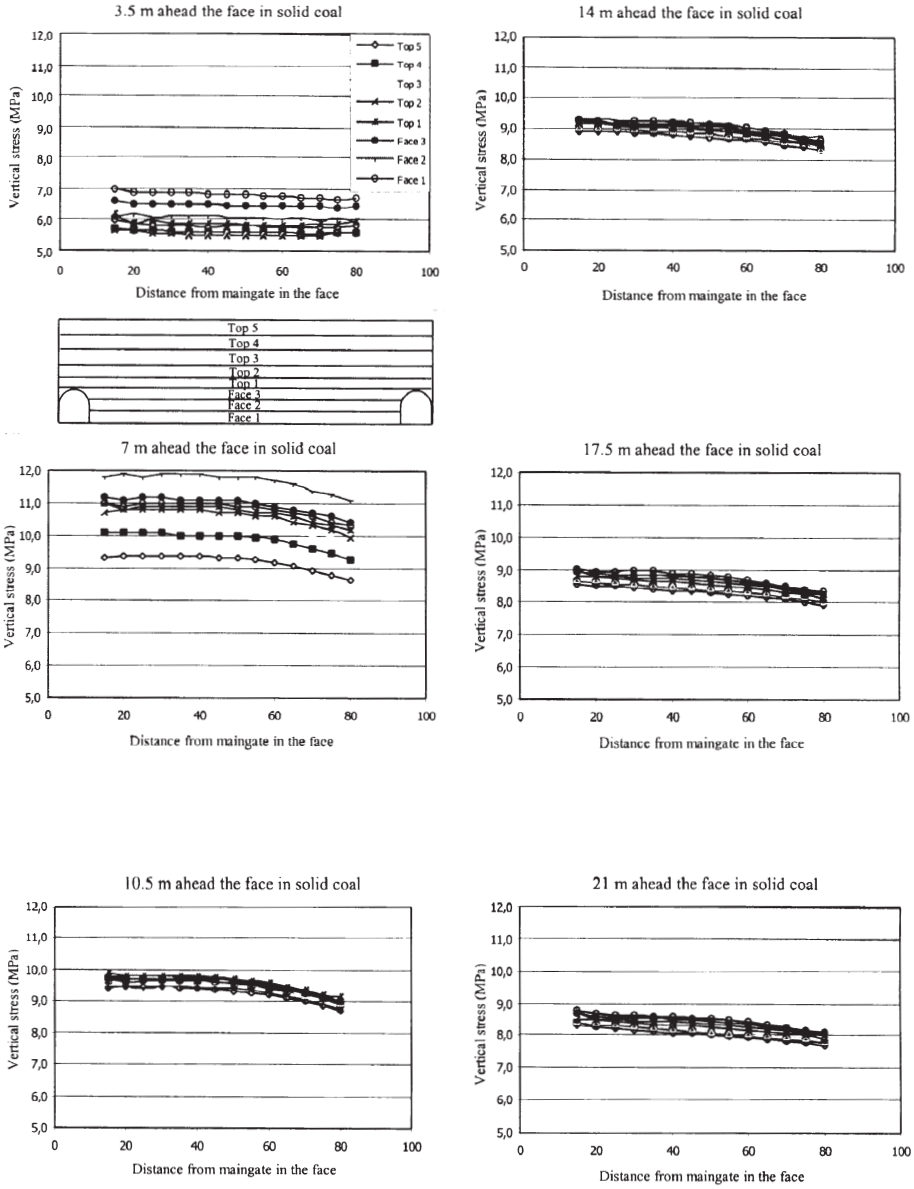

Figure 10—Vertical stress distribution around the face at various intervals perpendicular to face after 30 m advance from the face start line

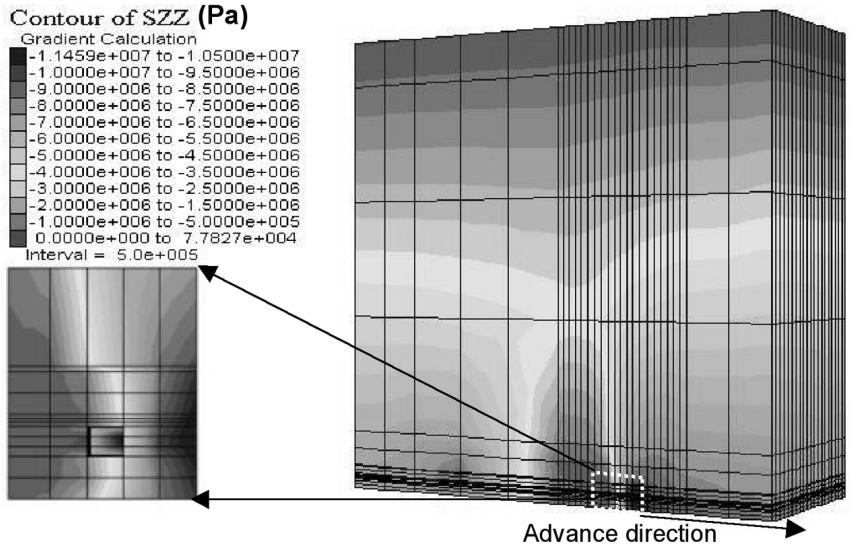

Figure 11—Vertical stresses distribution (z direction) after 60 m of face advance

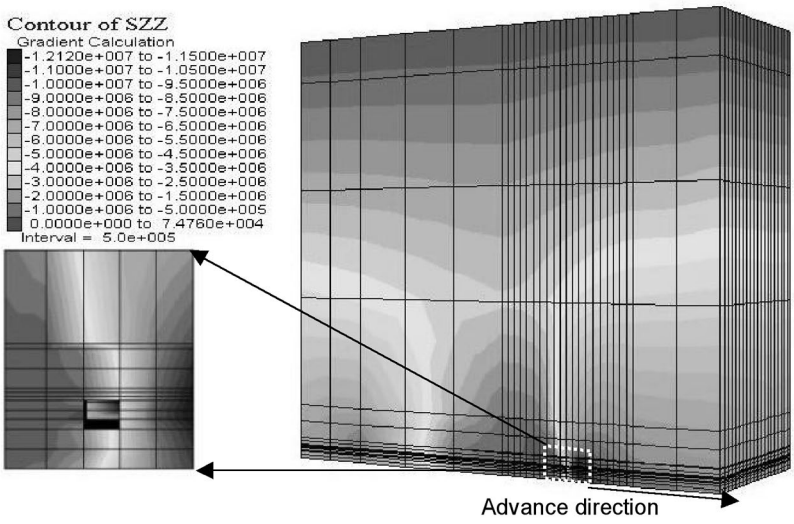

Figure 12—Vertical stresses distribution (z direction) after 90 m of face advance

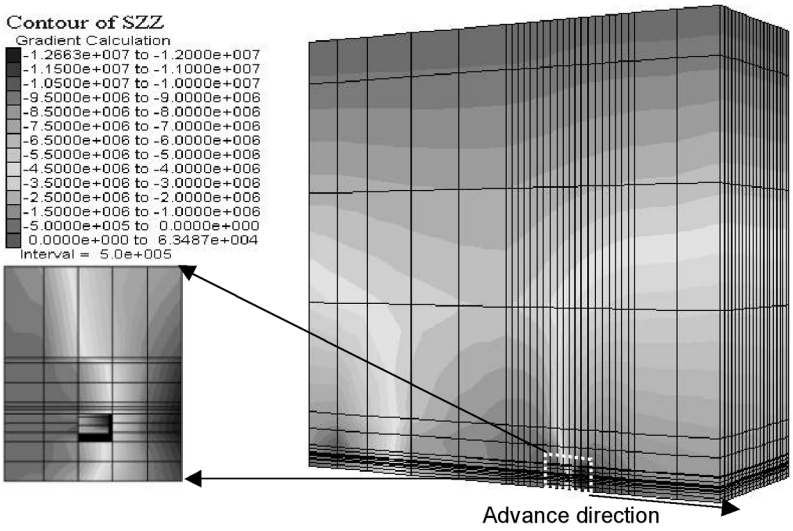

Figure 13—Vertical stresses distribution (z direction) after 120 m of face advance

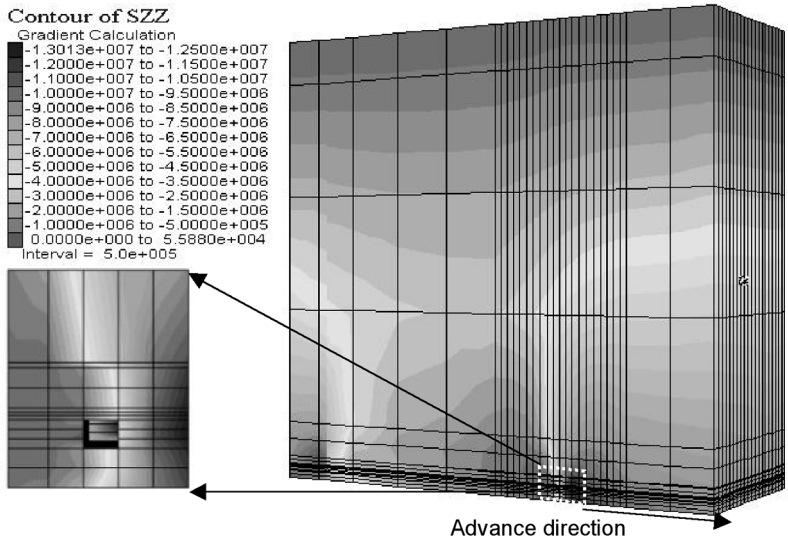

Figure 14—Vertical stresses distribution (z direction) after 150 m of face advance

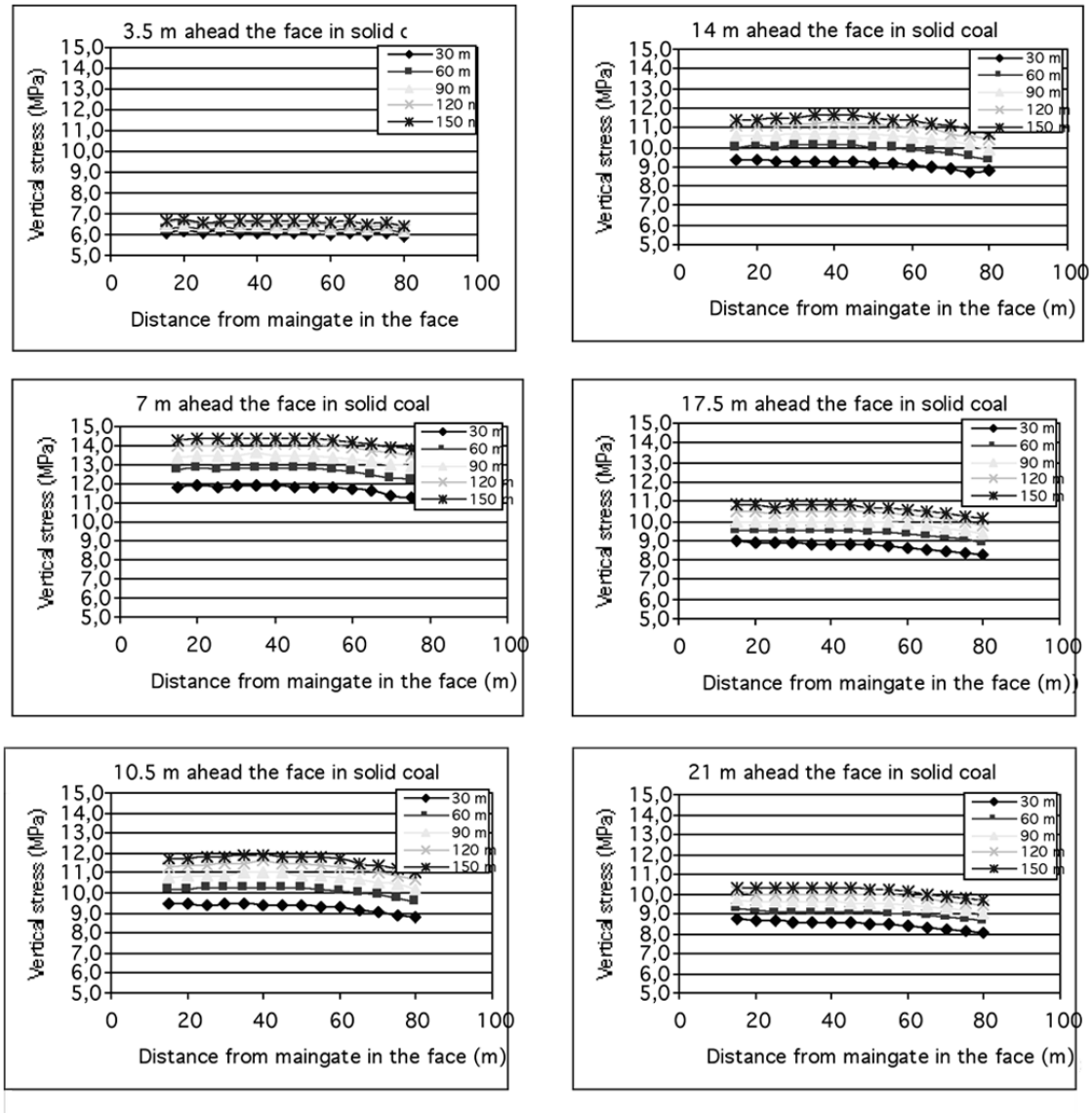

Figure 15—Vertical stresses distribution on axes parallel to the face at various distances after 30, 60, 90, 120 and 150 m of face advance from the face start line

Vertical stress distributions obtained from the model after 30, 60, 90, 120 and 150 metres of face advance from the face start line are presented in Figure 17. When Figure 16 and Figure 17 are compared, it is rather clear that characteristics of stress distributions obtained by means of numerical modelling are in a good agreement with the results of actual measurements in underground conditions. The magnitude of field stress was calculated as 5.75 MPa and presented with a dashed line in Figure 17.

Figure 17 was drawn to facilitate a comparison of numerical modelling results with stress distribution based on *in situ* measurements given in the literature. Front abutment stresses for various stages of face advance were superimposed. Rear abutment stresses for 30, 60, 90, 120 and 150 m of face advances from start line conditions are also shown in the figure. As shown in Figure 17, the front abutment pressure increases up to a distance of 7 m from the face line, reaching to a maximum stress level of 14.4 MPa. After reaching to the highest value, the front abutment pressure decreases gradually towards an initial field stress value of 5.75 MPa at a distance of approximately 70 m away from the face. As can be seen in Figure 17, the vertical front abutment stress at a further 70 m ahead of the face was about 7–8 MPa, whereas the field stress level was 5.75 MPa. This difference was attributed to the effect of the maingate and tailgate on the solid coal in front of the face since the M3 panel was produced by means of the retreat longwall method with a relatively short face length of 90 m. The abutment stress formed at a distance of 7 m in front of the face was found to increase 2.6-fold according to initial field stress. Stress in the goaf behind the face decreases to 0.1 MPa levels and tends to increase at the start line of the face in a manner similar to front abutment stresses. At the face start line of the panel, rear abutment stresses reach to the highest level at 2–3 m inside the solid coal and decrease gradually to the field stress level at about 60 m inside the solid coal.

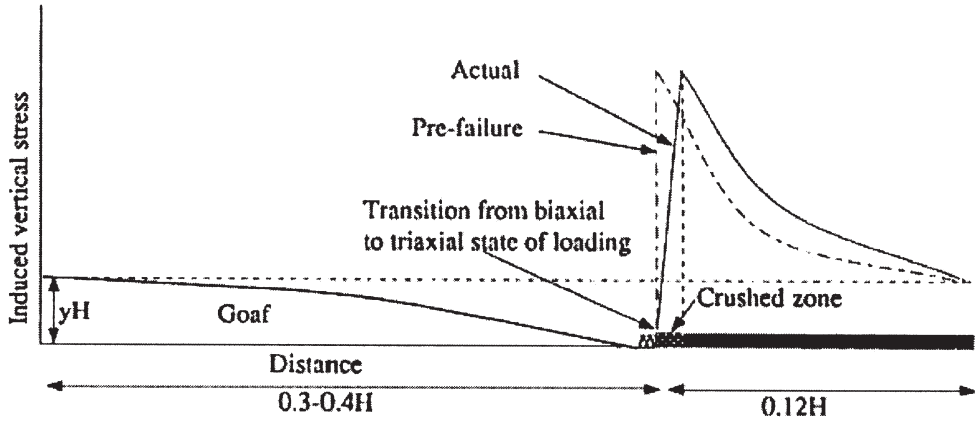

Figure 16—Stress redistribution around a longwall face given in literature based on *in situ* measurements[16–18]

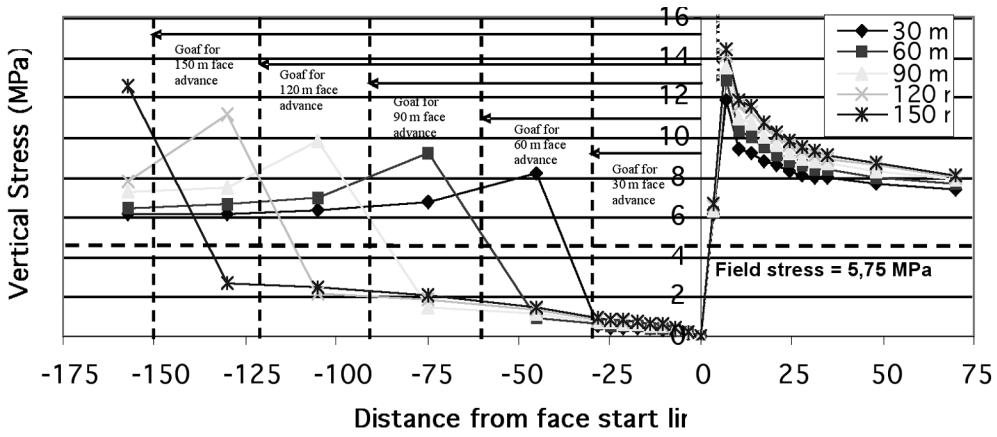

Figure 17—Vertical stresses found by numerical modelling around the face and goaf depending on face advance

Modelling of the longwall panel after five stages of face advance (30, 60, 90, 120 and 150 m) was unsatisfactory to reflect stress distribution in the *y* direction. Therefore, the model was further solved for face advances of 210 m and 270 m. Maximum front abutment stresses observed at 7 m ahead of the face for different stages of face advance can be seen in Figure 18. The results obtained from models reveal that the magnitude of vertical front abutment stress increased at a high rate up to a distance of 150 m of face advance from the face start line, whereas the rate of increase in the amount of front abutment stresses was slowed down after 200 m of face advance from the face start line. From this point forward, front abutment stress values tended to stay constant.

As mentioned earlier, the maximum front abutment stress was observed at 7 m ahead of the face in solid coal. However, an analysis of front abutment stresses at different parts of the coal-seam during production has shown that maximum front abutment stress was formed at various locations, depending on the distance between face and face start line. Maximum vertical front abutment stress regions for various conditions are presented in Figure 19.

Modelling of the M3 panel in 3-D has enabled determining the location of maximum vertical stress regions inside the coal-seam. Since the coal-seam was thick, stress distribution in front of the face at a specified distance was found variable along the seam between roof and floor.

Vertical abutment stresses have reached their maximum values at the Face 1 and Face 2 regions (see Figure 6) in general for various stages of face advance. For instance, irrespective of face advance from the face start line, the vertical abutment stress was observed in the Face 1 region in coal between 0 to 3.5 m and 14 to 21 m ahead of the face. Vertical abutment stress values observed for Face 2, Face 3 and Top Coal 1, 2, 3, 4 and 5 were lower than the Face 1 region. Between 3.5 to 7 and 10.5 to 14 m ahead of the face the maximum vertical stresses were formed in the Face 2 region. The location of maximum vertical stress at a distance between 7 and 10.5 m ahead of the face has changed depending on the distance of face advance from the face start line. The vertical stress has reached its maximum value at different levels in this region; after 30 and 60 m advance of face from the start line, the maximum vertical stress has taken place at the Top Coal 2 Region. However, as the face further advanced about 90 to 120 m, the location of maximum stress has shifted above the Top Coal 4 Region. After the face was advanced more than 150 m from the face start line, the maximum vertical stresses have taken place at Face 1 Region and Face 2 Region contact.

The changing character of the maximum vertical stress location in coal between 7 and 10.5 m ahead of the face can be attributed to the process of compaction of caved ground behind the face. Formation of goaf at the initial stage of face advance between 30 and 60 m from the face start line, the

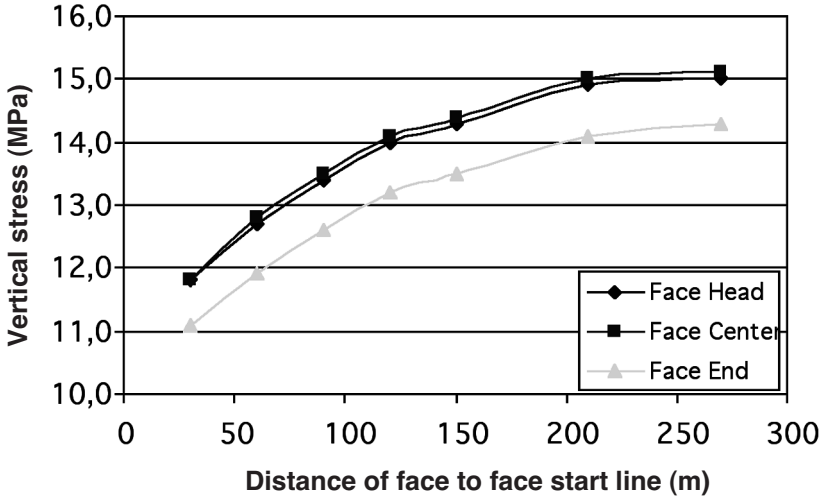

Figure 18—Maximum vertical stresses at 7 m in front of the face at various stages of face advance

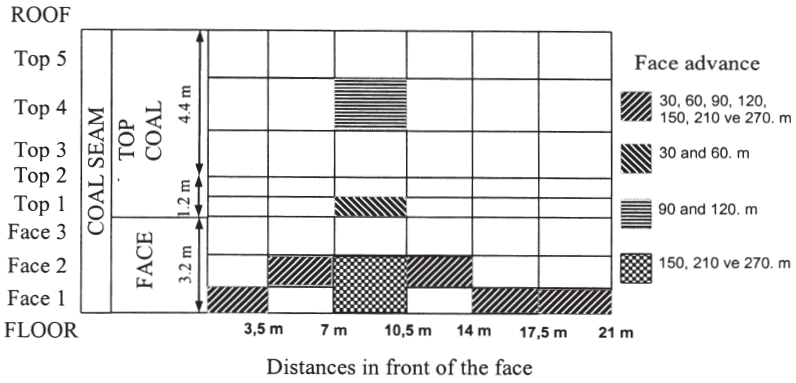

Figure 19—Maximum vertical stress zones in front of the face

void ratio was high. Caving of the main roof would not be completed until a face advance of 120 m. After this point, the main roof leaning on the goaf would be well established, leading to compaction of caved ground. Then, during this process, vertical stress would be formed at various levels in coal due to the cantilever effect of the roof strata.

Conclusions

In this study, the results of a comprehensive 3-D numerical modelling of a longwall panel at Omerler underground mine are presented. A sophisticated software called FLAC3D has been used for modelling. For realistic modelling of stresses and displacements, material properties were derived for the rock mass from the laboratory data by using Hoek-Brown failure criterion, RMR and GSI system, together with empirical equations.

Modelling results have shown that stresses around longwall faces could be successfully modelled by using FLAC3D. Results revealed that maximum vertical abutment stresses (8.4–14.4 MPa) were formed at a distance of 7 m in front of the face. After reaching the highest value, the front abutment pressure gradually decreased towards the initial field stress of 5.75 MPa at a distance of 70 m from the face. Stresses in around the face and goaf decreased to 0.1 MPa levels and tended to increase to the initial field stress level in the goaf towards the face start line. Characteristics of stress distribution found by numerical modelling coincided with the results given in the literature by means of *in situ* measurements.

Complexity of the underground operations related to thick seam coalmining requires the use of 3-D modelling. Modelling in 2-D cannot be considered as adequate for a longwall panel together with its surroundings. The results presented in this paper are part of a comprehensive research programme carried out for modelling of stress-displacement distribution around longwall faces in thick seam mining and modelling of caving characteristics of top coal behind the face.

It can be confidently put forward that stresses and displacement calculated by numerical modelling were in good agreement with *in situ* observations in the mine. Therefore, the results of numerical models are validated with the general conditions observed in the mine. It is believed that numerical modelling results presented in this paper will facilitate the understanding of strata behaviour around retreat longwall faces.

Acknowledgements

The results of this paper are based on a science and research project funded by Hacettepe University, Scientific Researches Unit. The authors are obliged to Dr. Fatih Bulent Taskin for providing help during the field trials. Thanks are due to the management of the Turkish Coal Enterprise and Omerler Colliery for their valuable co-operation during field observations.

References

1. Taskin, F.B. Optimum dimensioning of pillars between longwall panels in Tuncbilek Mine, Ph.D Thesis, Osmangazi University, Eskisehir, 1999, p. 149 (in Turkish).
2. Destanoglu, N., Taskin, F.B., Tastepe, M., and Ogretmen, S. *Application of GLI Tuncbilek-Omerler underground mechanisation*, Ankara: Kozan Publishing, Ankara, 2000. p. 211. (in Turkish)
3. Yasitli, N.E. Numerical modelling of longwall with top coal caving. MSc. Thesis, Hacettepe University, Ankara, 2002, p. 148 (in Turkish).
4. Itasca, User manual for FLAC3D, Ver. 2.0, Itasca Consulting Group Inc., Minnesota, 1997.
5. Hoek, E. and Brown, E.T. Practical estimates of rock mass strength. *Int. J. of Rock Mech. Min. Sci.*, 1997, vol. 34, no. 8, pp. 1165–1186.
6. Bieniawski, Z.T. Engineering classification of jointed rock masses. Trans S. *Afr. Inst.Civ. Eng.*, 1973, vol. 15, pp. 335–344.
7. Bieniawski, Z.T. *Engineering rock mass classifcations: a complete manual for engineers and geologists in mining, civil and petroleum engineering*. New York: Wiley, 1989. pp. 251.
8. Hoek, E. Strength of rock and rock masses. *ISRM News Journal,* 1995; vol. 2, no.2, pp. 4–16.
9. Sonmez, H. Investigation on the applicability of the Hoek-Brown criteria to the failure of the fissured clays. Ph.D. Thesis, Hacettepe University, Ankara, 2001, p. 215 (in Turkish).
10. Sonmez, H. and Ulusay, R. Modifications to the Geological Strength Index (GSI) and their applicability to stability of slopes, *Int. J. of Roch Mech. and Min. Sci.*, 1999, vol. 36, no. 6, pp. 743–760.
11. Unver, B. and Yasitli, N.E. The Simulation of sublevel caving method using in thick coal seam by computer. Hacettepe University Scientific Research Unit, Project No: 00 02 602 008, 2002, p. 148 (in Turkish).
12. Yasitli, N.E. and Unver, B. 2003, 3-D estimation of stresses around a longwall face by using finite difference method, *18th International Mining Congress of Turkey*, Antalya, 2003, pp. 83–88.
13. Xie, H., Chen, Z., and Wang, J. Three-dimensional numerical analysis of deformation and failure during top coal caving, Int. *J. of Rock Mech. Min. Sci.*, 1999, vol. 36, no. 6, pp. 651–658.
14. Kose, H. and Cebi, Y. Investigation the stresses forming during production of thick coal seam, *6th Coal Congress of Turkey*, Zonguldak, 1988, pp. 371-383.
15. Yavuz, H. and Fowell, R.J. Softening effect of coal on the design of yield pillars. In FLAC and Numerical Modeling in Geomechanics, *Proc. of The 2nd International FLAC Conference*, Lyon, France, D. Billaux *et al.*(eds.), Lisse: A. A. Balkema, 2001, pp. 313–320.
16. Singh, R., Mandal, P.K., Singh, A.K., and Singh, T.N. Cable-bolting-based semi-mechanised depillaring of a thick coal seam. Int. *J. of Rock Mech. Min. Sci.,* 2001, vol. 38, pp. 245–257.
17. Sheorey, P.R. Design of coal pillar arrays and chain pillars. *Comprehensive rock engineering*. vol. 2, Oxford, Pergamon Press, 1993.
18. Wilson, A.H. Pillar stability in longwall mining. In: Chugh Y.P., Karmis M., (eds). *State of the art of ground control in longwall mining science.* New York, SME, 1982. pp. 85–95. ◆